Aerodynamic Properties of a Two-Dimensional Inextensible Flexible Airfoil

S. Greenhalgh*
Naval Air Development Center, Warminster, Pennsylvania
and
H. C. Curtiss Jr.† and B. Smith‡
Princeton University, Princeton, New Jersey

The results of experimental and theoretical studies of the aerodynamic characteristics of a two-dimensional inextensible flexible airfoil are presented. Experiments included measurement of the lift, drag, and membrane tension forces acting on a single-surface mylar membrane supported by elliptical rods at the leading and trailing edges. A unique method of measuring membrane tension was developed which allowed the tension to be determined experimentally. A theoretical study was conducted that produced a simpler formulation of the problem than is found in the literature. Theoretical results are in good agreement with experimental data for those angles of attack where the flow over the membrane is not separated. All of the membranes exhibited maximum lift-to-drag ratios near zero angle of attack. The measured lift-to-drag ratios are comparable to conventional rigid airfoils. Hysteresis of the membrane airfoil near zero angle of attack was observed experimentally.

Nomenclature

$\{a\}$ = column matrix with p elements, $= \{0,0,0\ldots -p\alpha\}^T$
a_{ij} = aerodynamic influence coefficient, $= 1/[1+2(i-j)]$
$[A]$ = matrix of aerodynamic influence coefficients, $= [a_{ij}]$
c = chord of airfoil
$[C]$, $[E]$, $[H^*]$, $[G^*]$ = matrices defined in Table 2
C_ℓ = lift coefficient, $= L/\frac{1}{2}\rho U^2 c$
C_T = tension coefficient, $= T/\frac{1}{2}\rho U^2 c$
$[I]$ = unit diagonal matrix
L = lift on airfoil per unit width
ℓ = membrane length
p = number of airfoil segments
T = tension in membrane per unit width
U = freestream velocity
$\bar{x}$ = horizontal location on membrane, nondimensionalized by chord
XL = nondimensional membrane excess length $= [(\ell - c)/c] \times 100$
$\bar{y}$ = vertical displacement of membrane, nondimensionalized by chord
$2p\delta_i$ = nondimensional curvature of element i, $d^2\bar{y}/d\bar{x}^2$, $\delta_i = \frac{1}{2}(\theta_i - \theta_{i-1})$
α = airfoil angle of attack
β_i = one-half nondimensional curvature of element i, $= p\delta_i$
γ_i = vortex strength per unit length on element, $= (p/c)\Gamma_i$
γ_i^* = nondimensional vortex strength, γ_i/U
Γ_i = line vortex strength on element i
ΔC_{p_i} = pressure coefficient of element i, $= \Delta p_i/[\rho(U^2/2)]$
Δp_i = pressure difference across element i
θ_i = slope at trailing edge of element i
θ_i' = slope at trailing edge of element i relative to freestream velocity direction
θ_{i-1} = slope at leading edge of element i
ρ = density of air
ψ_i = average slope of element i, $d\bar{y}/d\bar{x}$, $\psi_i = \frac{1}{2}(\theta_i + \theta_{i-1})$
ψ_i' = average slope of element i relative to freestream velocity direction, $= \psi_i - \alpha$

Introduction

THE theory of the two-dimensional lifting membrane has been the subject of a number of investigations.[1-4] Thwaites[1] used linearized thin airfoil theory to relate the membrane shape to membrane loading to obtain an integrodifferential equation, "the sail equation," which he then solved using matrix methods. Nielsen's[2] solution to the problem was based on Fourier series and numerical techniques. Both Thwaites and Nielsen obtained an eigenvalue problem. The Nielsen paper refers to limited wind tunnel tests. Chambers[3] applied variational methods to Thwaites' sail equation considering only the eigenvalue problem. Jackson,[4] in a recent paper discussing the effects of elasticity on a two-dimensional sail, showed that major portions of Nielsen's results can be closely approximated by representing the membrane shape empirically by a simple cubic relationship. Ormiston[5] undertook a thorough investigation of the Princeton Sailwing, a double-membrane airfoil with a tubular leading edge and a taut wire trailing edge. He presents both theoretical and experimental results for a three-dimensional Sailwing. However, there is a lack of experimental data on single-surface membrance airfoils. This study was undertaken to experimentally determine the aerodynamic characteristics together with the shape and tension data for a two-dimensional inextensible membrance airfoil.

Experimental data were obtained for several membranes over a range of excess material lengths and angles of attack.

Presented as Paper 83-1796 at the AIAA Applied Aerodynamics Conference, Danvers, Mass., July 13-15, 1983; submitted Aug. 4, 1983; revision received Nov. 7, 1983.

*Aerospace Engineer. Member AIAA.
†Professor, Department of Mechanical and Aerospace Engineering. Member AIAA.
‡Graduate Student, Department of Mechanical and Aerospace Engineering.

Table 1 Experimental apparatus

Model:	30.5 cm wide × 45.7 cm long × 1 mm thick mylar membrane supported on two elliptical rods that were free to rotate about their respective axes.
Wind tunnel:	The Princeton University Two-Dimensional Subsonic Facility 0.305 m wide × 1.22 m high test section.
Test conditions:	
Angle of attack, α	-20 deg $\leq \alpha \leq 20$ deg
Excess length, XL	$0 \leq XL < 5.7$
Camber (nominal)	0-15.5%
Dynamic pressure (nominal)	7.7 N/m^2
Reynolds number	1.3×10^6

The excess material length of the membrane is defined as the difference between the length of the membrane and the chord, nondimensionalized by the chord length and expressed in percent.

The excess length can be approximately related to the percent camber of the airfoil by using the result for a symmetric parabolic arc which gives $t/c = 6.1\sqrt{XL}$. Since the membrane shape depends upon the test conditions in these experiments, all results are presented in terms of the experimentally measured quantity, the excess length.

Measurements were made of lift, drag, and membrane tension as a function of the excess length and angle of attack.

Airfoil lift was determined by measurement of the pressure distribution induced on the tunnel floor and ceiling. Drag was obtained from the momentum deficiency in the wake as measured with a drag rake. Tension was measured employing a strain gage implanted in the membrane.

An optical system was developed to photograph the aerodynamically loaded membrane. Experimentally determined membrane shapes were compared to the predicted shapes over the total range of tests.

The wind tunnel test results will be presented first, followed by a discussion of the theory. Then a comparison will be made between theory and experiment. Finally, some qualitative observations on oscillatory behavior of the membrane which was observed in various test conditions will be presented.

Wind Tunnel Experiments

The tests were conducted in a two-dimensional wind tunnel. The model and wind tunnel characteristics are given in Table 1.

Preliminary studies were conducted in a low-speed two-dimensional smoke tunnel to determine the sensitivity of the airfoil characteristics to several of the physical variables.[6]

Figures 1 and 2 present some of the experimental data obtained from the tests. Figure 1 shows the lift coefficient variation with angle of attack for various excess lengths. The family of lift curves shows that increasing the excess length of the membrane produces an upward displacement of the lift curve. This is a consequence of a larger excess length producing increased airfoil camber. It is also interesting to observe that the membranes produce positive lift at negative angles of attack for all of the excess lengths tested. Limit cycle oscillations of the membrane were also observed at negative angles of attack, particularly for the larger excess lengths as described later in this paper.

It was found from the experiments that when the excess length of the membrane is greater than approximately 2%, the lift curve slope above $\alpha = 0$ deg decreases as the excess length increases. Flow visualization studies utilizing tufts indicate that flow separation is the cause of this decrease in the lift curve slope.

These airfoils exhibit a benign stall behavior. The location of the maximum camber point on the flexible airfoil moves forward with increasing angle of attack tending to compensate for separation on the trailing edge. Separation is accompanied by small-amplitude vibration of the membrane.

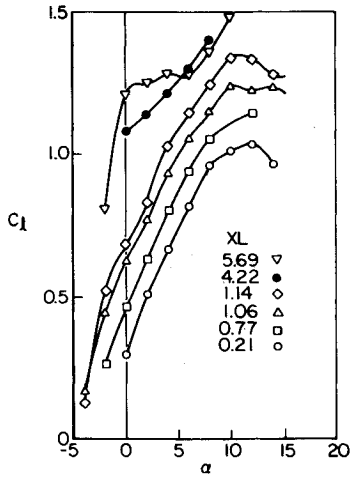

Fig. 1 Measured lift coefficient vs angle of attack for various excess lengths.

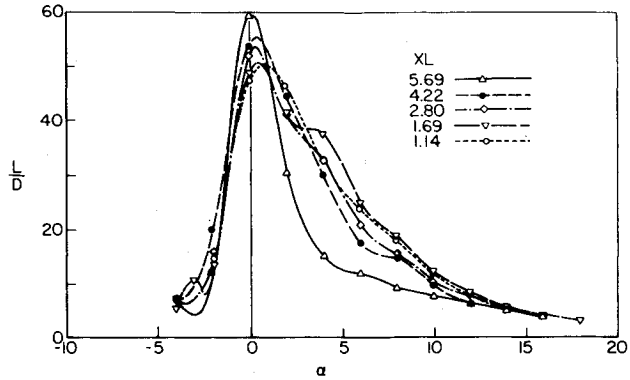

Fig. 2 Measured lift-to-drag ratio vs angle of attack for various excess lengths.

Figure 2 shows the variation in lift-to-drag ratio with angle of attack for various excess lengths. The maximum lift-to-drag ratio occurs near zero angle of attack and increases with excess length. The airfoil with an excess length of 5.69% exhibits a very narrow range of high lift-to-drag ratio. The large lift-to-drag ratio is a consequence of the high lift produced by the large camber at zero angle of attack together with the low drag value. The sharpness of this curve is associated with a narrow drag bucket around zero angle of attack at larger excess lengths. The minimum measured value of the drag coefficient is equal to 0.015. It occurs at zero angle of attack and was found to be essentially independent of excess length.

Theory

The theoretical approach to the problem of calculating the lift, pressure distribution, and shape of a two-dimensional airfoil whose lifting surface is an inextensible membrane is described.

The basic formulation consists of simultaneous solution of an aerodynamic equation describing the relationship between the vorticity distribution on a two-dimensional airfoil and the shape of the airfoil and a structural equation describing the relationship between the shape of the membrane and the loading on the membrane. The first equation is taken directly from thin-airfoil theory[7] and the second equation is obtained from a balance of forces on the membrane. The second equation also can be viewed as the equation for the bending of a plate in the limiting case of zero flexural stiffness.[8]

In addition to these two equations there is an additional relationship or constraint which must be applied. In terms of the physical system, i.e., the manner in which the wind tunnel experiments were conducted, this constraint is the length of the flexible membrane. The solution to this formulation of the problem is found in the literature.[1,2] However, this approach is quite complex since introduction of the length constraint makes the resulting set of governing equations nonlinear. A considerably simpler formulation of the problem is obtained by choosing a value for the tension in the membrane. Then, the simultaneous solution of the aerodynamic and structural equations in discrete form is obtained by solving a set of simultaneous linear algebraic equations, a much simpler task. Then, once this solution has been obtained, the length of the membrane can be calculated directly.

The governing equations are presented in discrete form suitable for solution on a digital computer. The membrane is broken into p segments of length c/p. A line vortex of strength Γ_i is located at $\frac{1}{4}c/p$ from the leading edge of each segment, and the flow boundary condition is satisfied at a control point located at $\frac{3}{4}c/p$ from the leading edge of the element. It has been shown that this spacing of the collocation points produces rapid convergence and does not require external imposition of the trailing-edge Kutta condition.[9] The aerodynamic equation is

$$-\pi\psi_i' = a_{ij}\gamma_j^* \tag{1}$$

where

$$a_{ij} = \frac{1}{1+2(i-j)} \tag{2}$$

The average slope of element i with respect to the freestream direction is,

$$\psi_i' = \frac{1}{2}(\theta_i' + \theta_{i-1}') = \left.\frac{d\bar{y}}{d\bar{x}}\right|_i - \alpha \tag{3}$$

A nondimensional vortex element strength has been introduced as

$$\gamma_i^* = p(\Gamma_i/Uc) \tag{4}$$

The pressure difference across the airfoil at any chordwise location can be expressed in terms of the vortex strength from the Kutta-Joukowski law,

$$\Delta C_{p_i} = 2\gamma_i^* \tag{5}$$

Balancing forces on an element of the membrane yields a relationship between the pressure difference, the curvature of the element, and the tension in the membrane. In nondimensional form

$$\Delta C_{p_i} = -2C_T\beta_i \tag{6}$$

The nondimensional curvature of element i is

$$\beta_i = p\frac{1}{2}(\theta_i' - \theta_{i-1}') = \frac{1}{2}\left.\frac{d^2\bar{y}}{d\bar{x}^2}\right|_i$$

Equations (5) and (6) can be combined to give

$$\gamma_i^* = -C_T\beta_i \tag{7}$$

Now Eqs. (1), (3), (4), and (7) can be solved simultaneously with the additional condition that the trailing edge of the airfoil is on the x axis. The resulting equations in matrix notation are

$$[A]\{\gamma_i^*\} = -\pi\{\psi_i'\} \tag{8}$$

$$\{\gamma_i^*\} = -C_T\{\beta_i\} \tag{9}$$

$$\sum_{i=1}^{p}\psi_i' = -p\alpha \tag{10}$$

$$\{\psi_i'\} = \tfrac{1}{2}[C]\{\theta_j'\} \tag{11}$$

$$\{\beta_i\} = -(p/2)[E]\{\theta_j'\} \tag{12}$$

We can also combine Eqs. (10-12) by eliminating θ_j' and defining the new matrices H^* and G^*, so that,

$$[A]\{\gamma_i^*\} + \pi\{\psi_i'\} = 0 \tag{13}$$

$$\{\gamma_i^*\} + C_T\{\beta_i\} = 0 \tag{14}$$

$$[H^*]\{\psi_i'\} + (1/p)[G^*]\{\beta_i\} = \{a\} \tag{15}$$

where H^* and G^* are as defined in Table 2.

This set of equations can be solved after choosing the number of segments p, the angle of attack α, and the tension coefficient C_T. Then the pressure coefficient on the airfoil is obtained from Eq. (5) and the lift coefficient is determined by

$$C_\ell = \frac{1}{p}\sum_{i=1}^{p} 2\gamma_i^* \tag{16}$$

The excess length can be expressed in terms of the local slope and angle of attack as

$$\left(\frac{XL}{100}\right) = \frac{1}{2p}\sum_{i=1}^{p}\psi_i'^2 - \frac{\alpha^2}{2} \tag{17}$$

The excess length is determined from Eq. (17) after Eqs. (13-15) have been solved. The approaches found in the literature consider the tension as unknown and proceed to solve Eqs. (13-15) simultaneously with Eq. (17). This can be seen to be a much more complex approach due to the nonlinear character of Eq. (17).

One special case of interest is the solution to this set of equations when the angle of attack is zero. In this case Eqs. (13-15) are homogeneous and the value of C_T cannot be specified a priori. In this case it is convenient to combine these equations since finding specific values of C_T is an eigenvalue problem. Equations (13-15) can be combined to yield the following equation:

$$[C_T[I] + (\pi/p)[H^*]^{-1}[G^*][A]^{-1}]\{\psi_i'\} = -C_T[H^*]^{-1}\{a\} \tag{18}$$

Equation (18) is now expressed in such a form that the eigenvalues of C_T for the case in which the angle of attack equals zero can be readily calculated.

Calculations with these equations indicate that the solution converges relatively rapidly and that 20 segments are sufficient to obtain accurate results. With some experience it is quite straightforward to find solutions for given values of the excess length corresponding to the manner in which the experiments were performed.

Comparison between Theory and Experiment

Figure 3 is a comparison between theory and experiment for the lift coefficient for values of excess length XL of 0.21, 0.77, and 1.14%. Comparison is not shown for the larger excess lengths of Fig. 1 since for these cases the flow over the airfoil is separated over most of the range of angle of attack. The theoretical curves have been biased by 1 deg to account

Table 2 Definition of matrices

$[C]$ = matrix with $p+1$ columns, p rows,

$$\begin{bmatrix} 1 & 1 & 0 & 0 & \ldots & & \\ 0 & 1 & 1 & 0 & 0\ldots & & \\ 0 & 0 & 1 & 1 & 0\ldots & & \\ \vdots & & & & & & \\ 0 & 0 & 0 & 0 & 0\ldots & 1 & 1 \end{bmatrix}$$

$[E]$ = matrix with $p+1$ columns, p rows,

$$\begin{bmatrix} 1 & -1 & 0 & 0 & \ldots & & \\ 0 & 1 & -1 & 0 & \ldots & & \\ 0 & 0 & 1 & -1 & 0\ldots & & \\ \vdots & & & & & & \\ 0 & 0 & 0 & 0 & 0\ldots & 1 & -1 \end{bmatrix}$$

$[G^*] = p \times p$ matrix,

$$\begin{bmatrix} 1 & 1 & 0 & 0\ldots\ldots \\ 0 & 1 & 1 & 0\ldots\ldots \\ 0 & 0 & 1 & 1\ldots\ldots \\ \vdots & & & \\ 0 & 0 & 0 & 0\ 0\ldots\ 0 \end{bmatrix}$$

$[H^*] = p \times p$ matrix,

$$\begin{bmatrix} 1 & -1 & 0 & 0 & 0\ldots \\ 0 & 1 & -1 & 0 & 0\ldots \\ 0 & 0 & 1 & -1 & 0\ldots \\ \vdots & & & & \\ 1 & 1 & 1 & 1 & 1\ldots\ 1 \end{bmatrix}$$

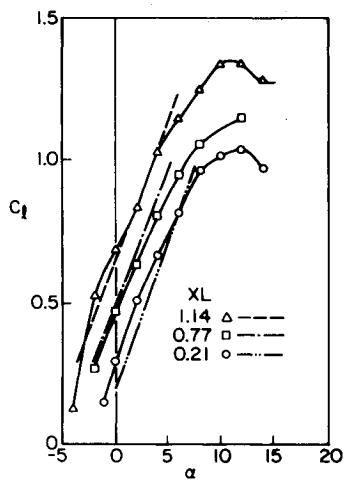

Fig. 3 Comparison of theory and experiment. Lift coefficient vs angle of attack for various excess lengths.

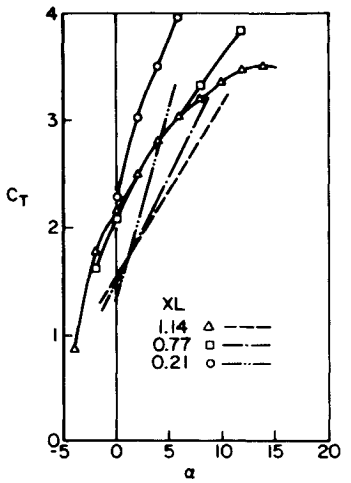

Fig. 4 Comparison of theory and experiment. Tension coefficient vs angle of attack for various excess lengths.

for the measured flow angularity in the wind tunnel. The lift coefficient agrees very well with theory with differences less than approximately 5% provided the angle of attack lies in the range of -5 to $+8$ deg.

It was found from the computational results that C_ℓ could be approximated in the following form:

$$C_\ell \cong 2\pi\alpha \pm 0.1\,B(XL)^{1/2}$$

The form of the result is the same as found by Thwaites and Nielsen. Thwaites determined B to have the value of 6.36, and Nielsen a value of 7.2784. In the present study B was found to be closely approximated as 7.0.

The lift produced by a two-dimensional flexible membrane exceeds the lift of a flat plate by an amount expressed approximately by $0.7\,(XL)^{1/2}$. This empirical constant is smaller than the value that would be obtained for a symmetric parabolic arc (7.7) because the maximum camber point is forward of the midchord at positive angle of attack.

Figure 4 illustrates the comparison between experiment and theory for the tension coefficient variation with angle of attack and excess length. The values of the measured tension

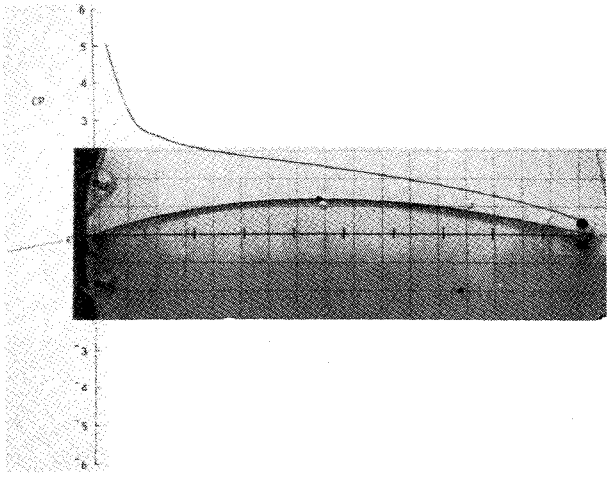

Fig. 5 Comparison of theory and experiment. Membrane shape $\alpha = 10$ deg, $XL = 1.16$.

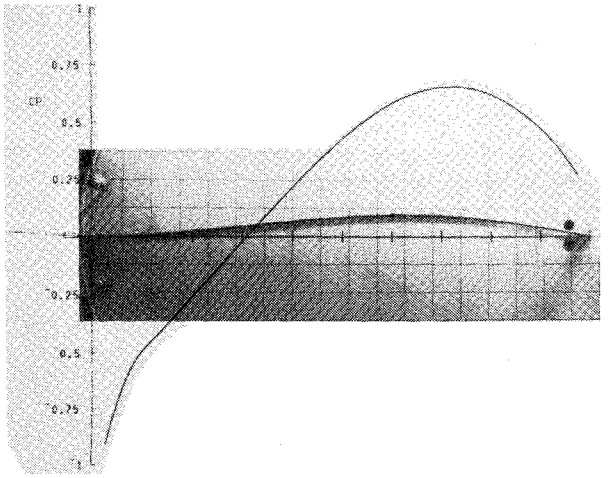

Fig. 6 Comparison of theory and experiment. Membrane shape $\alpha = -3$ deg, $XL = 0.45$.

coefficients are larger than the theory predicts; however, the variation with angle of attack is predicted by theory.

For tension coefficients larger than 1, an approximate relationship between the tension coefficient, the excess length, and the angle of attack is

$$C_T = 1.73 \pm 9.1\alpha\,(XL)^{-1/2}$$

The value of the tension coefficient C_T corresponding to zero angle of attack is the smallest eigenvalue of Eq. (18). The experimental results indicate a value of 2.1 at zero angle of attack.

The predicted shapes show that the point of maximum camber is forward of the midchord point for high angles of attack and moves aft toward the midpoint as the angle of attack is reduced. At zero angle of attack the membrane shape is symmetrical about the midchord point. For negative angles of attack, an inflection point develops near the leading edge of the membrane and the point of maximum camber moves from the center of the membrane toward the trailing edge.

Comparison of the theoretical shapes with the experimental membrane shapes indicates good agreement over the range of values of excess length and angle of attack examined in these experiments. Figures 5 and 6 are composite pictures of the theoretical profiles and experimental membrane shapes where the computer-developed profile is superimposed on a photograph of the aerodynamically loaded membrane photographed in the wind tunnel. Also shown are the predicted pressure distributions associated with the test condition.

If the angle of attack is less than zero, the membrane shape possesses an inflection point located at the point where the pressure coefficient is equal to zero. This is evident from the theoretical development, since the curvature of the membrane is directly proportional to the pressure difference across the membrane.

Under certain operating conditions when the magnitude of the angle of attack is less than some critical value, multiple lift coefficients are possible at the same angle of attack and excess length.

This behavior was observed experimentally. At a large positive angle of attack the membrane forms a convex profile producing positive lift. As the angle of attack is decreased below zero, an inflection point develops in the profile forming a concave/convex surface. The membrane in this condition still produces positive lift. If the angle of attack is decreased further past a critical negative value, the membrane pops through and assumes a single inverted shape producing negative lift. This inverted convex shape of course is the same in every respect as its positive counterpart . Now, if the angle of attack change is reversed and the airfoil moved to a positive angle of attack, the reflexed shape again forms until a critical positive angle is exceeded and the membrane pops through to a positive lift condition.

The theory also predicts the existence of multiple lift coefficients for a single angle of attack in agreement with this experimentally observed hysteresis loop that appears in the curves of lift and tension coefficient variation with angle of attack. However, only two values of lift coefficient were observed experimentally.

Figures 7 and 8 compare theory and experiment for the lift coefficient C_ℓ and the tension coefficient C_T as a function of angle of attack in the range where hysteresis occurs. The theoretical prediction of the hysteresis loops agrees well with experiment.

The appearance of hysteresis in the theory can be seen from Fig. 9 which shows the predicted variation of the tension coefficient with excess length for various constant values of angle of attack. There is a critical value of the magnitude of the angle of attack for a given excess length corresponding to the point where $\partial XL/\partial C_T = 0$ ($C_T = 0.902$). For a given excess length, if the magnitude of the angle of attack is smaller than this critical value, then there are multiple solutions for the tension coefficient and corresponding multiple solutions for the lift coefficient. The membrane shape is convex if the tension coefficient is greater than the eigenvalue, and has one or more inflection points for tension coefficients smaller than this value. For an angle-of-attack magnitude larger than the critical value there is only a single solution for $C_T > 1.727$. Thus the hysteresis behavior can be seen from the following argument. At a given excess length, as the angle of attack is reduced from some positive value to a negative value, first the region where multiple solutions exist is encountered. A further reduction in the angle of attack to the critical point where tension coefficient equals 0.902 corresponds to the maximum negative angle of attack for which a solution exists. Further reduction in angle of attack results in a pop-through of the membrane to a solution with $C_T > 1.727$. Experimentally the membrane popped through at a C_T value closer to unity, somewhat larger than at the predicted value of 0.902.

Figure 9 also shows that a larger excess length produces a larger hysteresis loop since larger opposite sign angles of attack are possible before pop-through occurs.

As mentioned earlier in this paper, various limit cycle oscillations of the membrane were associated with the behavior of the membrane near the pop-through point. Preliminary wind tunnel tests indicate a nodal point at about

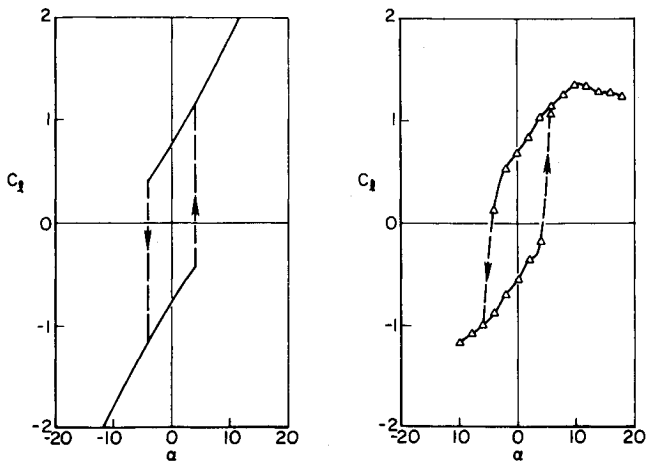

Fig. 7 Comparison of theory and experiment. Lift hysteresis, $XL = 1.14$.

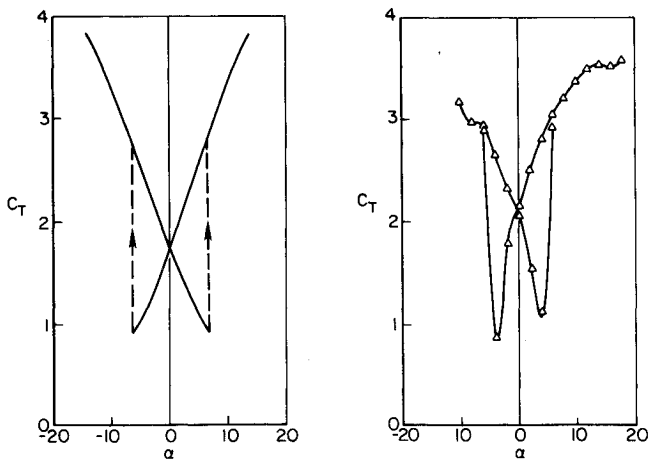

Fig. 8 Comparison of theory and experiment. Tension hysteresis, $XL = 1.14$.

60% chord of the oscillating membrane. Further, the intensity and frequency of the oscillation depended on excess length, the magnitude of the angle of attack, and the tunnel dynamic pressure. Figure 10 shows the approximate regions where oscillations were observed in these tests. The oscillations were particularly evident at the larger excess lengths. Stroboscopic observations of the airfoil indicated that the frequency band is relatively narrow for a fixed set of conditions. However, the change of frequency with angle of attack is quite dramatic and the frequency approaches zero just before the pop-through point occurs. Also the intensity of the dynamic motion as indicated by the amplitude of the oscillation and the noise generated increases rapidly soon after the system crosses the zero angle of attack. Finally it reaches a peak at an angle of attack of approximately 3 deg and, then, decreases slowly as the pop-through point is reached.

Conclusions

1) The operating range of a membrane airfoil is limited by stall and separation at high angles of attack and by hysteresis phenomena at low angles of attack.

2) The angle of attack at which separation occurs decreased with increasing excess length and the hysteresis range increases resulting in a narrow operating range for the highest excess lengths examined.

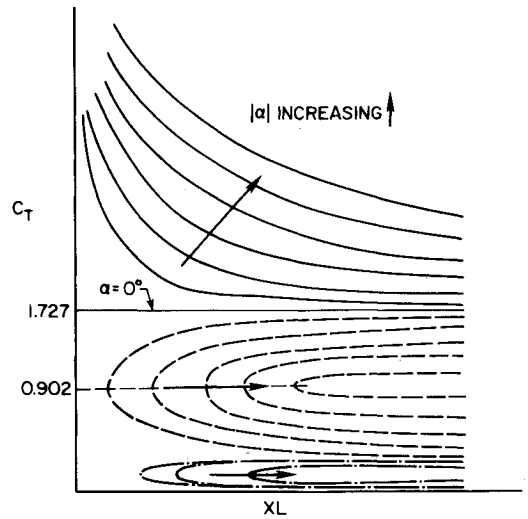

Fig. 9 Tension coefficient vs excess length for various angles of attack, theory.

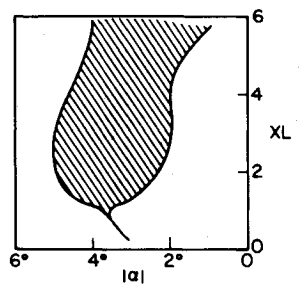

Fig. 10 Experimentally observed limit cycle boundaries.

3) For all of the membranes tested a benign stall was observed.

4) A membrane airfoil can exhibit positive lift over a range of negative angles of attack which depends on the excess length. Membrane oscillations are also observed in this regime at larger excess lengths.

5) A convenient theoretical approach to the problem is presented which agrees well with the experimental results and previous analytical work.

References

[1] Thwaites, B., "The Aerodynamic Theory of Sails, I, Two-Dimensional Sails," *Proceedings of the Royal Society*, Ser. A, No. 1306, Vol. 261, May 16, 1961, pp. 402-422.

[2] Nielsen, J.N., " Theory of Flexible Aerodynamic Surfaces," *Journal of Applied Mechanics*, Vol. 30, Sept. 1963, pp. 435-442.

[3] Chambers, L.I., "A Variational Formulation of the Thwaites Sail Equation," *Quarterly Journal on Mechanical and Applied Mathematics*, Vol. 19, May 1966, pp. 221-231.

[4] Jackson, P., "A Simple Model for Elastic Two-Dimensional Sails," *AIAA Journal*, Vol. 21, Jan. 1983, pp. 153-155.

[5] Ormiston, R.A., "Theoretical and Experimental Aerodynamics of an Elastic Sailwing," Ph.D. Thesis, Princeton University, Princeton, N.J., Oct. 1969.

[6] Greenhalgh, S., "The Two-Dimensional Inextensible Lifting Membrane Airfoil-Theory and Experiment," NADC IR Rept. CG 123, Feb. 1983.

[7] Kuethe, A.M. and Chow, C-Y., *Foundations of Aerodynamics*, John Wiley and Sons, New York, 1976.

[8] Timoshenko, S. and Woinowsky-Kreiger, S., *Theory of Plates and Shells*, McGraw-Hill, Book Co., New York, 1959.

[9] James, R.M., "On the Remarkable Accuracy of the Vortex Lattice Method," *Computer Methods in Applied Mechanics and Engineering*, Vol. 1, June 1972, pp. 59-79.